Published by :
http://www.ijert.org

International Journal of Engineering Research & Technology (IJERT)
ISSN: 2278-0181
Vol. 10 Issue 05, May-2021

Self-Sustained Robot

Shantanu Kolekar
Department of Mechatronics Engineering
SSPU, Pune, Maharashtra, India

Sourav Jadhav
Department of Mechatronics Engineering
SSPU, Pune, Maharashtra, India

Jatan Limbasiya
Department of Mechatronics Engineering
SSPU, Pune, Maharashtra, India

***Abstract*- This research paper engages the reader to understand nuances of the design process of the self-sustained robot used in autonomous exploration, including link design, component selection, and active suspension algorithm which stabilizes the chassis horizontally that surpasses the compared algorithms to accomplish the desired result. On Solid works, Static analysis was performed to track the simulated undulating surfaces for the robot to move on. Structural analysis to ensure the prototype could perform as desired.**

Keywords – Self-Sustained Robot, Active Suspension, Structural Analysis, Arduino.

I. INTRODUCTION

Self-Sustained Robot provides good ride quality, handling, maintains road holding ability, and supports unvarying weight [1]. To enhance ride quality and safety, many researchers have analyzed different types of suspension systems, from passive, semi-active, to active ones. The conventional suspension system is uncomplicated and well-grounded, but its performance is unsatisfactory. A Semi-active system is better than a conventional suspension, but it has inadequate ability to meet high-performance demands [2]. The active suspension has drawn much attention in recent years because of its potential to meet tight performance requirements demanded by consumers, it can improve the ride quality and maintain good handling and road holding simultaneously [3].

Our main purpose is to develop an innovative and smart electronically controlled self-sustained system that always stabilizes the chassis to make it horizontal. The vehicle must be able to go over both smooth surfaces and sharp obstacles and should be able to detect lanes and obstacles in its path and traverse it with accuracy to reach its destination without accidents or damage to the components mounted on its chassis.

II. LINK DESIGN

We began by choosing an appropriate design for the link mechanism. Some of these were noticeable after discussions–

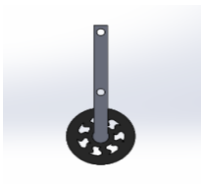

Figure 1

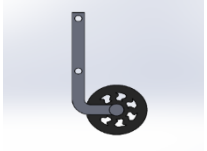

Figure 2

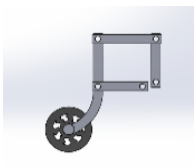

Figure 3

Fig 1. : Straight link (1 D.O.F.)

Fig 2. : L-link (1 D.O.F)

Fig 3. : Modified four-bar linkage

The Degree of Freedom using the Gruebler's criterion and other criterions were considered [4].

$$F = 3(N - 1) - 2P1 - P2 = 1$$

where, N = 4; P1= 4; P2= 0

Various advantages and disadvantages of the designs were weighed upon and based on the design with the right amount of robustness and effectiveness was chosen. The straight link seemed ideal for the purpose but was eliminated solely due to the fact the all the force on the link will directly act on the servo which could harm it. The L-link was effective but did not have efficacy. The modified four-bar was finally chosen and further analysis and calculations were done.

III. COMPONENT SELECTION

A. MPU-6050 (Inertial Measurement Unit)

MPU 6050 is an inertial measurement unit (IMU) is an electronic device that measures and reports a body's velocity, orientation, and gravitational forces, using a combination of accelerometers, gyroscopes and magnetometers.

The main purpose of an IMU in our project is to get the absolute angular orientation of the chassis. This data would be fed to the microcontroller which will take action in case there is a disturbance in the orientation. We chose the IMU MPU-6050 for our purpose as it was accurate to about 0.01 degree and was cheap.

Some useful product specifications from its datasheet [5] are as follows –

a) Digital-output X-, Y-, and Z-Axis angular rate sensors (gyroscopes) with a user programmable full scale range of ±250, ±500, ±1000, and ±2000°/sec.
b) Integrated 16-bit ADCs enable simultaneous sampling of gyros
c) Improved low-frequency noise performance
d) Digitally-programmable low-pass filter
e) Gyroscope operating current: 3.6mA

International Journal of Engineering Research & Technology (IJERT)
ISSN: 2278-0181
Vol. 10 Issue 05, May-2021

f) An embedded temperature sensor and an on-chip oscillator with ±1% variation over the operating temperature range .

Figure 4 MPU 6050

B. Servo Motor

Maximum Payload that the robot could lift was found to be 6 kg, by performing a structural analysis on SolidWorks. This meant that each link had to bear a load of 1.5 kg., at 90 degrees the torques on the servo is maximum
i.e., 1.5kg x 5.8cm = 8.7 kg-cm = 0.087kg-m.
The following servo motor was bought as it satisfies our requirements and the company is reputed and verified by previous experiences.
Servo name: Tower Pro MG995 [6]
Operating speed @ (6.0V): 0.11sec/60°
Stall torque @ (6.0V): 9.45kg-cm (= 0.0945 kg.m)
Weight 44g

Figure 5 Servo Motor

C. DC Geared Motor

Our application, i.e. planetary exploration requires low land speeds (0.14 kmph for rover). For a wheel with 68mm diameter, RPM required to attain a similar speed is 10RPM. Motor selected: geared DC motor (100 RPM)
Specifications –

- 100 RPM 12V DC motors with Gearbox.
- 125gm weight.
- Rated Torque: 1.2 Kg-cm
- Load Current: 0.3 A

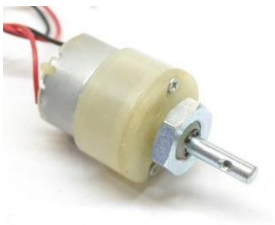

Figure 6 DC Motor

D. Controller ATmega328P

An ATmega328 Microcontroller was chosen for the project. The primary reasons were its abundant availability on Arduino Uno boards, experience and ease of use. The technical specifications [7] are listed in the table (Table 1) below.

Table 1 Specifications of ATmega328P

Operating Voltage	5V
Input Voltage	7-12v
Digital I/O pins	14 (of which 6 are PWM)
DC current for digital I/O pin	40mA
Flash Memory	32KB
Clock Speed	16 MHz

Figure 7 Arduino Uno

IV. ACTIVE SUSPENSION ALGORITHM

Purely kinematic based suspension systems are not accurate enough, therefore a controlled kinematic suspension system would be perfect[8]. The suspension system must have “auto-stabilization” which means it must be able to recover from all sorts of unprecedented actuations due to rough terrain.

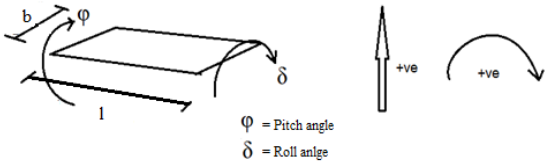

Figure 8 Pictorial Representation

Pitch angle = φ
Roll angle = δ

For Pitch correction,

Servo Actuation (Δθp) =
(Δθp) = $(\varphi + \tan^{-1}(d/l)) * (\theta max) / (\tan^{-1}(d/l)) - \theta max$

For Roll correction,

Servo actuation
(Δθr) = (Δθp) = $(\delta + \tan^{-1}(d/b)) * (\theta max) / (\tan^{-1}(d/b)) - \theta max$

l = tyre centre to tyre centre length (in cm)
b = tyre centre to tyre centre breadth (in cm)
d = the maximum possible bump that can be overcome by the suspension system (in cm)

With no suspension, the maximum pitch angle subtended by chassis is $\tan^{-1}(d/l)$.
Similarly, the maximum roll angle subtended by the chassis is $\tan^{-1}(d/b)$.

International Journal of Engineering Research & Technology (IJERT)
ISSN: 2278-0181
Vol. 10 Issue 05, May-2021

To correct this instability, the maximum servo deflection is θmax. On linearly mapping the maximum chassis deflection to maximum servo angles we form a relation to auto-stabilize the chassis even when it is in the worst possible case.

Independent corrections are required as pitch and roll corrections are independent as they are at right angles. For Servo motors assuming actuation upwards as positive and other negative, Table 2 elaborates the servo actuations.

Table 2 Tabulated actuations for servo motors

Actuation	Pitching up/down and roll right	Pitching up/down and roll left
Left tyre	$\theta_{current} = \theta_{current} - \Delta\theta_p - \Delta\theta_r$	$\theta_{current} = \theta_{current} - \Delta\theta_p$
Right tyre	$\theta_{current} = \theta_{current} - \Delta\theta_p$	$\theta_{current} = \theta_{current} - \Delta\theta_p + \Delta\theta_r$

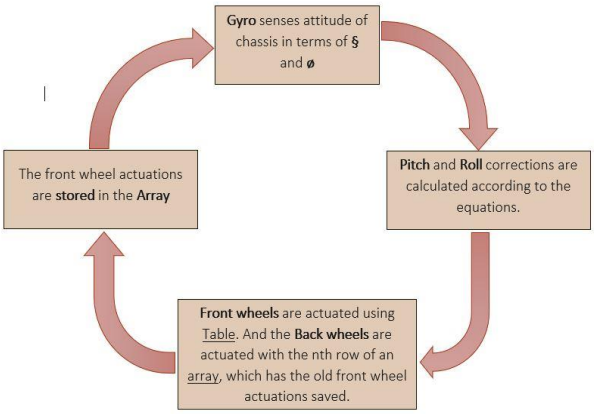

Figure 9 Flow Chart of Active Suspension Algorithm

A very important point to note here is that the two back tyres have to go through the same path that the front two tyres followed and hence they just have to mimic the front two tyres' actuations, but after a lag. This lag depends on how fast the robot is moving, i.e., after how long the rear wheels reach the same obstacle as the front tyres did. This can be done by storing the servo actuations in an array and executing the nth array actuation for back tyres. The whole process can therefore be summed up in the following flow chart (Fig. 9) which depicts the flow of events inside the microcontroller.

V. SIMULATION AND ANALYSIS

A. *Isometric View*

From this view, one can get the clear understanding of how links are assembled and components are placed.

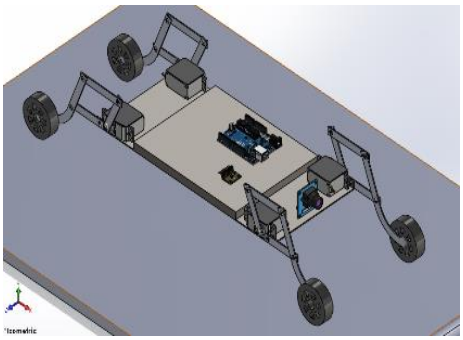

Figure 10 Isometric View

B. *Observations*

1. *Wheel trace and chassis trace*

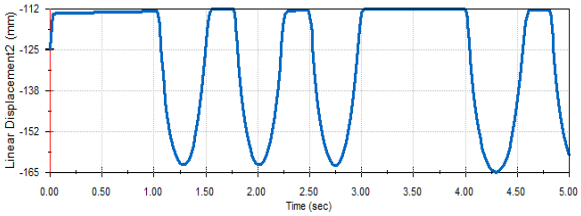

Figure 11 Wheel Trace

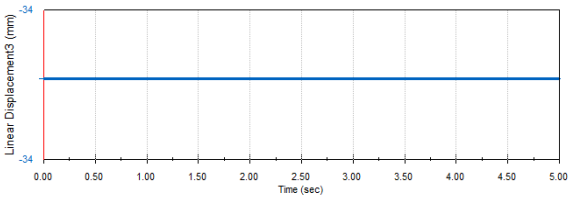

Figure 12 Chassis Trace

Wheel trace (Fig. 11) and chasis trace (Fig. 12) indicates the movement of system going over the bumper in which the chasis remains horizontal/parallel and reflects almost negligible error. Thus achieving our purpose.

2. *Structural Analysis*

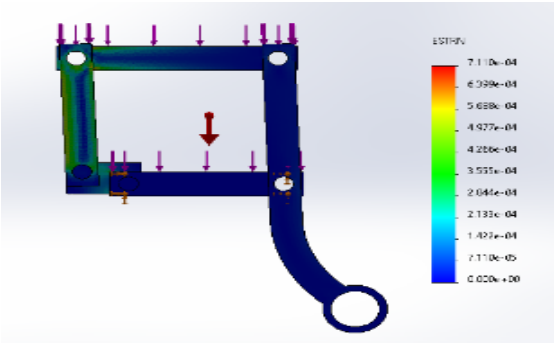

Figure 13 Stress Analysis of Four bar

Static structural analysis using Solid Works was performed on the link to see how much deflection and how much stress is developed on the application of the different amount of forces to find out the payload carrying capacity of the link.

International Journal of Engineering Research & Technology (IJERT)
ISSN: 2278-0181
Vol. 10 Issue 05, May-2021

The material for simulation is SS (Stainless Steel) as all our links were supposed to be Laser Cutted, their properties are as follows

a) Modulus of Elasticity = 19299 N/mm2
b) Density = 8000 Kg/m3
c) Ultimate Tensile Stress = 580 N/mm2
d) Yield Stress = 172 N/mm2
e) Poisson's Ratio = 0.27

The robot can therefore lift loads to 6 kg. This weight also includes the robot's weight. On actual testing of limits after prototyping, the robot could safely lift a total of 5892 gm. Robot weight = 1969 gm Additional payload = 3923 gm. At this weight servo motors and links had reached their limit and started to deform and twist. This result was consistent with all the Simulations performed on Solid-Works.

3. Displacement, velocity and acceleration curve

Below table & graphs indicate the displacement , velocity and acceleration of the links with respect to time.

Table 3 Kinematics of links

Time (s)	Displacement (mm)	Velocity (mm/s)	Acceleration (mm/s²)
0	-7.084	4.34*E-15	445.39
0.00833	-7.075	3.148	444.69
0.01666	-7.048	7.393	151.85
0.025	-7.004	11.032	432.672
0.0333	-6.942	14.623	427.901

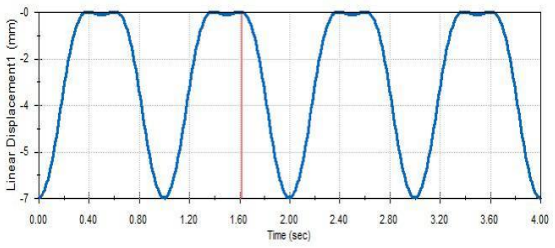

Figure 14 Displacement vs time curve

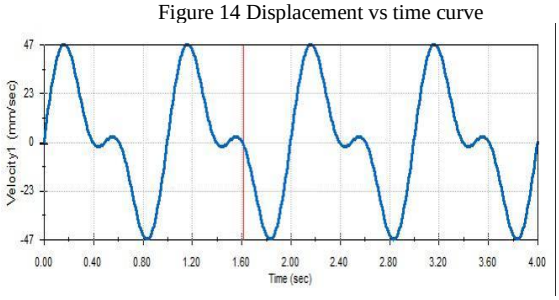

Figure 15 Velocity vs time curve

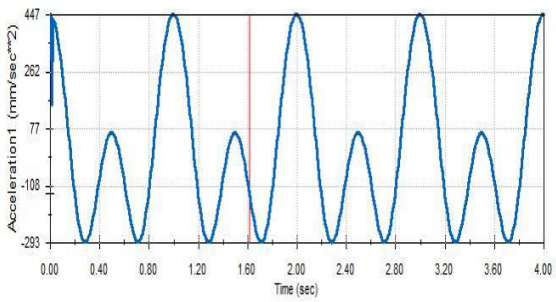

Figure 16 Acceleration vs time curve

VI. CONCLUSION

The primary goal of designing a self-sustained robot that endures a nearly horizontal chassis regardless of terrains was accomplished. Based on the robot that we have built, it can successfully go over a smooth bump and climb a stair that is at most 5cm high. The negative feedback loop gives the best results as compared to passive suspension systems, which is way more than designed. Also, the algorithm designed resulted in auto–stabilization and recovery from any angle, something which was not intended to be one of the objectives, to begin with. This system is designed for a slow-moving robot as most space exploration robots are slow-moving in nature. The same system may not work as efficiently for a fast-moving robot. Thus it is important to note that robots with this system should ideally not be used for high-speed operations. The prototype that we have created did not have a motor driving circuit or a steering mechanism as they were both beyond the objective of the project. It is important to not exceed the rated voltage of the various electronic devices as it would lead to their failure which will result in the failure of the robot.

ACKNOWLEDGMENT

We would express our most profound and sincere gratitude to our guide, Prof. Ganesh Lohar of Mechatronics Engineering, his support and continuous encouragement throughout the project. Without his guidance and persistent help, this research would not have been possible. We must acknowledge the Director and faculties of the school of Mechatronics Engineering for providing fresh perspectives on the topic, which in turn helped me enhance our skills.

REFERENCES

[1] Rajamani, R., 2011. *Vehicle dynamics and control*. Springer Science & Business Media.

[2] John H. Crews, Michael G. Mattson, Gregory D. Buckner, "Multi-objective control optimization for semi-active vehicle suspensions," Journal of Sound and Vibration, Volume 330, Pages 5502–5516, 2011

[3] Sy Dzung Nguyena, Quoc Hung Nguyenb, Seung-Bok Choi, " A hybrid clustering based fuzzy structure for vibration control - An application to semi-active vehicle seat-suspension system," Mechanical Systems and Signal Processing Volumes 56–57, Pages 288–301, 2015.

[4] Renzi, C. and Leali, F., 2016. A multicriteria decision-making application to the conceptual design of mechanical components. *Journal of multi-criteria decision analysis*, *23*(3-4), pp.87-111.

[5] MPU 6050 Datasheet - http://www.invensense.com/mems/gyro/documents/PS-MPU6000A-00v3.4.pdf 36

[6] https://www.alldatasheet.com/datasheet-pdf/pdf/1132435/ETC2/MG995.html

[7] Arduino Uno Technical overview http://www.arduino.cc/en/Main/ArduinoBoardUno

[8] Tani, K., Matsumoto, O., Kajita, S. and Shirai, N., WHEELEDROBOTS TO OVERCOME GROUND UNEVENNESS IN CONSTRUCTION AREAS.

[9] Li, P., Lam, J. and Cheung, K.C., 2014. Multi-objective control for active vehicle suspension with wheelbase preview. *Journal of Sound and Vibration*, *333*(21), pp.5269-5282.

International Journal of Engineering Research & Technology (IJERT)
ISSN: 2278-0181
Vol. 10 Issue 05, May-2021

[10] Hsieh, M.F. and Ozguner, U., 2008, June. A parking algorithm for an autonomous vehicle. In *2008 IEEE Intelligent Vehicles Symposium* (pp. 1155-1160). IEEE.

[11] Park, M., Lee, S. and Han, W., 2015. Development of Steering Control System for Autonomous Vehicle Using Geometry-Based Path Tracking Algorithm. *Etri Journal*, *37*(3), pp.617-625.

[12] Shi, Q. and Zhang, H., 2020. Fault diagnosis of an autonomous vehicle with an improved SVM algorithm subject to unbalanced datasets. *IEEE Transactions on Industrial Electronics*.

[13] Park, M.W., Lee, S.W. and Han, W.Y., 2014, October. Development of lateral control system for autonomous vehicle based on adaptive pure pursuit algorithm. In *2014 14th International Conference on Control, Automation and Systems (ICCAS 2014)* (pp. 1443-1447). IEEE.

[14] Yan, F., Dridi, M. and El Moudni, A., 2013. An autonomous vehicle sequencing problem at intersections: A genetic algorithm approach. *International Journal of Applied Mathematics and Computer Science*, *23*(1), pp.183-200.

[15] Mars Pathfinder: www.mpf.jpl.nasa.gov